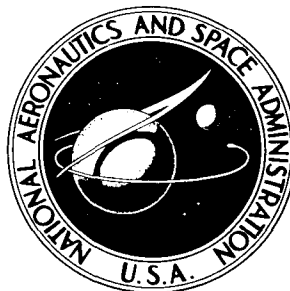


CASE FILE  
COPY

NASA TECHNICAL NOTE



NASA TN D-2155

NASA TN D-2155

✓

THE SHAPE OF A MAGNETICALLY ROTATED  
ELECTRIC ARC COLUMN IN AN ANNULAR GAP

*by James R. Jedlicka*

*Ames Research Center*

*Moffett Field, Calif.*

THE SHAPE OF A MAGNETICALLY ROTATED ELECTRIC ARC  
COLUMN IN AN ANNULAR GAP

By James R. Jedlicka

Ames Research Center  
Moffett Field, Calif.

NATIONAL AERONAUTICS AND SPACE ADMINISTRATION

---

For sale by the Office of Technical Services, Department of Commerce,  
Washington, D.C. 20230 -- Price \$0.75

# THE SHAPE OF A MAGNETICALLY ROTATED ELECTRIC ARC

## COLUMN IN AN ANNULAR GAP

By James R. Jedlicka

Ames Research Center  
Moffett Field, Calif.

### SUMMARY

An electric arc discharge whirled in the annular gap between concentric, cylindrical electrodes by an external axial magnetic field is analyzed. A simplified model of the system is chosen, such that the arc is replaced by an impenetrable, conducting cylinder moving in a uniform fluid. At equilibrium the arc axis assumes a shape in which the driving electromagnetic force balances the retarding fluid-dynamic force. The equation for the shape is demonstrated to be the involute of a circle. For large magnetic field strengths, "diffuse discharge" operation is predicted. Comparison with experiment is good. Finally, the interpretation of arc photographs is discussed.

### INTRODUCTION

Certain high-energy gas sources currently in operation consist of high-current electric arcs whirled between concentric electrodes by means of axial magnetic fields. The rapid motion of the arc roots along the electrodes minimizes electrode evaporation. Photographs with short-duration exposure show the discharge as a spoke, spiral-like, or a complete field of uniform light, depending upon values of the various experimental parameters.

To understand the discharge phenomenon, it is desirable to develop an equation for the shape of the discharge. It is not feasible to solve the MHD equations in three dimensions since one-dimensional flow solutions are just coming within grasp. Instead, severe simplifying assumptions are made here, and these can be finally justified only on the basis that certain aspects of the result appear to agree with experiment. The mathematical derivation herein follows quite closely that of V. Adams (ref. 1). The mathematical results are compared with photographic evidence regarding arc shape.

### SYMBOLS

|   |                          |
|---|--------------------------|
| b | effective arc diameter   |
| B | magnetic field intensity |

|             |   |
|-------------|---|
| c           | constant of integration   |
| $C_D$       | effective arc crossflow drag coefficient  |
| D           | aerodynamic crossflow drag force  |
| I           | arc current   |
| l           | arc length  |
| L           | Lorentz force   |
| p           | line segment in figure 4(b)   |
| r, $\theta$ | polar coordinates   |
| s           | minor radius of annular gap   |
| t           | major radius of annular gap   |
| x, y        | rectangular coordinates   |
| $\alpha$    | parameter for given operating conditions of the arc; defined by<br>$\alpha^2 = \frac{2BI}{C_D \rho b \omega_a^2}$ |
| $\rho$      | density   |
| $\phi$      | angle between the tangent to the arc curve at a point and the x axis  |
| $\omega_a$  | arc angular velocity with respect to fluid  |
| $\omega_f$  | fluid angular velocity with respect to stationary coordinates   |

#### ASSUMPTIONS

The problem is to determine the path of an electric-arc discharge occurring in the annular gap between concentric, cylindrical electrodes submerged in an externally applied magnetic field (fig. 1). In this section will be listed the basic assumptions required to make the problem mathematically simple, with explanation of their implications in several cases. There are seven assumptions which provide the basis for the mathematical derivation in the next section.

1. The arc column is represented as an impenetrable aerodynamic body having a crossflow drag coefficient,  $C_D$ , and a diameter, d, both invariant with arc length.

From a physical standpoint, if an arc is considered to be a region of very high temperature in a constant pressure environment of much lower temperature, the density in the arc column will be low compared to that in the surrounding region (see fig. 2). Most of the gas particles are therefore excluded from the arc column, and thus it approximates a solid obstacle which excludes all of the gas particles. This model of the arc is not original but, rather, appears to have first been presented in a 1958 paper by M. Angelopoulos (ref. 2, abstract translated in ref. 3).

The analogy between an arc and an impenetrable rod has been observed in arc experiments. In an unpublished experiment, N. Vojvodich of Ames Research Center obtained high-speed motion pictures of a magnetically spun electric arc having concentric electrodes. He noted that after initiation, the arc appeared to accelerate asymptotically to a limiting velocity which depended on magnetic field strength, as though it were a fan and DC motor combination. Moreover, vortices were observed in the wake of the arc, as would be expected from a rotating spoke (see fig. 3). Similarly, W. Carlson and W. Winovich of Ames Research Center monitored rotational speed as they changed the environmental pressure, and the experimental variation of speed with pressure was approximately that which would be predicted for a solid rod in crossflow; these data are used in reference 4. Schuette (ref. 5) found that when an arc is driven through a fluid at supersonic speeds, an observable bow shock wave is formed, and the measured pressure rise across the shock wave agrees with that predicted by the Rankine-Hugoniot relation (an abstract of ref. 5 is translated in ref. 3).

When a solid rod is assumed, the conservation equations of the arc region are bypassed, and the prediction of the arc path and size in terms of fluid and electrical properties can only be qualitative.

2. End effects at attachment points of the arc to the electrodes are negligible. The study is restricted thereby to large annular gaps. Experimental observation on what is a "large" gap is given in reference 1.

3. The arc exists as a continuous curve between the electrode surfaces. It will be demonstrated later that this assumption does not preclude occurrence of "diffuse discharges."

4. At steady state, the fluid rotates as a solid body having a constant angular velocity,  $\omega_f$ . This assumption would not be expected to hold in the vicinity of the confining walls (the electrodes) as pointed out in assumption 2, and it can be justified only on the basis of the resulting mathematical simplification.

5. The magnetic field intensity,  $B$ , and the fluid density,  $\rho$ , are everywhere constant outside the arc column.

6. The electric field between the electrodes produces negligible force on the arc column compared to that of the externally applied magnetic field. This assumption prevents the analysis from having meaning when the strength of the externally applied magnetic field is small, that is, when the force

on a charged particle due to the applied electrode voltage is large compared to the force of the externally applied magnetic field.

7. Fluid viscous effects are negligible except as they contribute to the crossflow aerodynamic drag.

#### DERIVATION OF THE ARC-SHAPE EQUATION

First the forces on a differential length of arc will be examined to deduce the necessary condition for steady state. Next, the kind of mathematical curve which satisfies the necessary condition will be developed. This section will be concluded by examining a special limiting case.

##### The Necessary Condition

As shown in figure 4(a), the arc is considered to take place in a plane normal to and lying between concentric, circular electrodes with the magnetic driving field perpendicular to this plane. If the coordinate system is imagined to rotate clockwise at angular velocity  $\omega_f + \omega_a$ , the arc will appear stationary in the  $x - y$  frame and the fluid will revolve counter-clockwise at angular speed  $\omega_a$  (see fig. 4(a)).

A differential length of arc,  $dl$ , will have an aerodynamic crossflow drag force  $D$ , acting at a right angle to the arc axis. The drag force can be expressed as the product of a crossflow drag coefficient,  $C_D$ , a crossflow fluid velocity,  $r\omega_a(dr/dl)$ , and a crossflow reference area,  $b dl$ .

$$D = C_D b dl \frac{1}{2} \rho \left( r\omega_a \frac{dr}{dl} \right)^2$$

On the same element of arc a Lorentz force will act:

$$L = BI dl$$

For steady state (no motion in the rotating coordinate system) these forces must be equal:

$$D = L$$

or

$$C_D b dl \frac{1}{2} \rho \left( r\omega_a \frac{dr}{dl} \right)^2 = BI dl$$

For given operating conditions  $B$ ,  $I$ ,  $C_D$ ,  $b$ ,  $\rho$ , and  $\omega_a$  are constant and can be lumped together. The above equation can then be written:

$$\left. \begin{aligned} r^2 \left( \frac{dr}{dl} \right)^2 &= \alpha^2 \\ \alpha^2 &= \frac{2BI}{C_D b \rho \omega_a^2} \end{aligned} \right\} \quad (1)$$

where

or

$$r \frac{dr}{dl} = \alpha \quad (2)$$

It can be seen from figure 4(a) that the following relationship will hold:

$$\frac{dr}{dl} = \cos(\varphi - \theta) = \cos \varphi \cos \theta + \sin \varphi \sin \theta$$

and

$$x = r \cos \theta$$

$$y = r \sin \theta$$

When these are substituted into equation (2),

$$x \cos \varphi + y \sin \varphi = \alpha \quad (3)$$

Equation (3) is a necessary condition which will now be shown to be satisfied, in general, by the involute of the circle of radius  $\alpha$ .

#### Demonstration That the Necessary Condition Is Satisfied by an Involute

Figure 4(a) has been redrawn with mathematical construction lines in figure 4(b). Here the arc describes a curve, a point on which is  $(x, y)$ , and the tangent line from the point makes an angle  $\varphi$  with the  $x$  axis. The normal to the curve at  $(x, y)$ , designated as line  $p$ , is constructed as is a line through the origin and parallel to the tangent line at  $(x, y)$ . Another line parallel to line  $p$  and passing through  $(x, 0)$  is also drawn.

From inspection of figure 4(b), one finds that the length of the line segment passing through the origin and terminating at line  $p$  consists of two segments,  $x \cos \varphi$  and  $y \sin \varphi$ . From equation (3)

$$x \cos \varphi + y \sin \varphi = \alpha$$

For a differential movement along the curve,  $d\ell$ ,  $p$  will increase by  $dp$  and  $\varphi$  by  $d\varphi$ . From figure 4(b)

$$dp = \alpha d\varphi$$

Integration yields

$$p = \alpha\varphi \quad (4)$$

plus a constant of integration which is zero if the curve is begun on the  $x$  axis at the point  $(\alpha, 0)$ , where  $\varphi$  is zero. Now construct dotted line segments  $\alpha\varphi \sin \varphi$  and  $\alpha \sin \varphi$ . From the figure one observes that

$$x = \alpha \cos \varphi + \alpha\varphi \sin \varphi$$

$$y = \alpha \sin \varphi - \alpha\varphi \cos \varphi \quad (5)$$

These are the parametric equations of an involute (see ref. 6), which mathematically is generated from circle of radius  $\alpha$ , the radius being composed of the physical quantities appearing in equation (1).

#### The Limiting Case

For the special case of  $\alpha \rightarrow 0$ , equation (3) becomes:

$$x \cos \varphi + y \sin \varphi = 0$$

or

$$\tan \varphi = - \frac{x}{y}$$

From figure 4(a) one finds

$$\tan \varphi = \frac{dy}{dx}$$

These equations may be combined to eliminate  $\tan \varphi$ :

$$\frac{dy}{dx} = - \frac{x}{y}$$



This can be integrated to yield:

$$\frac{x^2}{2} + \frac{y^2}{2} = c \quad (6)$$

Thus the arc path becomes a circle in the limiting case as  $\alpha \rightarrow 0$ .

## DISCUSSION

In the previous section it was found that within the limited framework of the assumptions, the path of the arc is the involute of a circle and a parameter,  $\alpha$ , was formed. In this section the significance of the parameter will be discussed, and then calculated and observed paths will be compared. The experimental evidence generally is in the form of photographs. No problems of interpretation exist when a discharge is well defined as a bright region surrounded by a dark one, as in figure 5(a). When this is not the case, interpretation is difficult, and the discussion will be concluded with some comment regarding the photography of electric arcs.

### The Parameter $\alpha$

Equation (1) defines the parameter,  $\alpha$ , in terms of physical quantities; in equation (5) it is seen also to represent the radius of the involute generating circle. One can, therefore, interpret the parameter,  $\alpha$ , from both a mathematical and a physical viewpoint.

Assumptions 2, 4, and 7 imply that the location of the electrodes has no effect on the shape of the arc path. This implication is consistent with equation (1) where physical electrode radii do not appear. It would seem, then, that electrode inner and outer radii could be arbitrarily chosen or changed without affecting the shape of the arc path. The choice cannot be completely arbitrary because mathematically the involute exists only outside of the generating circle of radius  $\alpha$ . Thus, if the arc path is to be an involute, a condition on the choice of inner electrode radius,  $s$ , is:

$$s > \alpha \quad (7)$$

From a physical standpoint, large values of  $\alpha$  would correspond to a weak magnetic field, a region of operation in which the effect of the electric field on the arc shape cannot be disregarded (assumption 6). The limiting case of zero magnetic field would produce a nonrotating arc in the radial direction, being governed completely by the electric field. It is apparent, then, that the present analysis is limited in significance to the condition of equation (7).

As indicated by the comments accompanying assumption 1, many of the quantities which make up the parameter,  $\alpha$ , in equation (1) are not easily measured experimentally, making evaluation of the parameter difficult. The quantities  $B$  and  $I$  are easily measured;  $\rho$  is more difficult; and  $b$ ,  $C_D$ , and  $\omega_a$  are idealized quantities. For purposes of discussion herein, the parameter will not be numerically evaluated. Instead, its dependence on  $B$  will be utilized.

In addition to the  $B$  which appears in equation (1) explicitly, one other quantity,  $\omega_a$ , is dependent on  $B$ . No data have been published giving measurements of the arc velocity with respect to the fluid,  $\omega_a$ . In an unpublished experiment, Vojvodich noted from high-speed motion pictures of a particular configuration that  $\omega_a$  appeared to be proportional to  $\omega_a + \omega_f$ . If the linear relationship is assumed to hold universally, the several published experiments giving  $\omega_a + \omega_f$  can be utilized to give the  $B$  dependency of  $\omega_a$ .

In references 1, 4, 7, 8, and 9, the fixed coordinate angular velocity is found to be dependent on  $B$  raised to powers less than unity, with considerable disagreement among the experimenters possibly caused by end effects in the vicinity of the electrodes. Only in reference 1 were the end effects recognized and avoided; the functional relationship was then found to be

$$\omega_a + \omega_f \sim B^{0.6}$$

If this value is substituted into equation (1), the following is found:

$$\alpha^2 \sim B^{-0.2} \quad (8)$$

From equation (8) it appears that the parameter,  $\alpha$ , diminishes slowly as the magnetic field,  $B$ , increases, a point which is not obvious from equation (1). This point will be used in the discussion which follows.

#### Comparison With Experiment

Several factors influence the appearance of the arc shape as observed by photography. The photography itself will be important, and this is discussed in the final section on arc photography. Photographs of low current arcs will offer the best possibility for comparison since the apparent arc diameter as seen on photographs will more nearly conform to the current-carrying region.

Similarly, the relative size of the electrodes will have a large effect on the appearance of the arc path. From equation (5) the shape predicted will depend only on the parameter,  $\alpha$ , and not on the electrode radii,  $a$

consequence of assumption 2. The only limitation offered by the simple theory is that of equation (7), in which the generating circle must be no larger than the inner electrode. The effect of electrode size on the appearance of the arc path is illustrated by the two solid curves of figures 6(a) and 6(b). The solid curves are identical involutes, produced by a generating circle of the same radius, and have identical outer electrode radii,  $t$ , but with much different inner electrode radii. It is obvious from the figures that appearance of the discharge will depend on relative electrode size. For a shape comparison, it is evident that a large ratio of outer to inner electrode radii,  $t/s$ , will be a better choice.

The effect of the magnetic field will be important in any comparison of arc shape from theory and experiment. If  $B$  is allowed to diminish toward zero, a point will be reached where assumption 6 will be violated because the force produced by the electric field will dominate and as a result the path will be a radial line. But under these conditions,  $\alpha$  would be larger than  $s$ , and mathematically the involute could not exist. As  $B$  is increased,  $\alpha$  will diminish (from eq. (8)) and the arc will twist more tightly. In figure 6(a) the dashed curve,  $t/\alpha = 49$ , can be compared with the solid curve  $t/\alpha = 10$ . A sufficient increase in magnetic field, for instance, should cause the arc to change from the solid to the dashed curve. For ordinary values of arc current, a photograph of an arc following the  $t/\alpha = 49$  curve should appear as a relatively uniform field of light, a point which will be considered in more detail in the section on the diffuse discharge.

Large gap configuration.- In the preceding section, it was pointed out that a large gap configuration with a small current discharge should offer the best opportunity for a comparison of theory with experiment. These conditions existed in the experiment of reference 10, a photograph of which is reproduced in figure 5(a). The curve of figure 5(b) has been drawn with the same  $s/t$  ratio and with the parameter  $\alpha$  chosen to give about the same number of revolutions of arc path as appears in figure 5(a). The agreement appears good and suggests that the basic assumptions may be reasonable.

Small gap configuration.- Figure 6(b) shows an outline of electrodes similar to that used in reference 4, wherein the gap is small compared to the outer electrode radius,  $t/s = 1.25$ . Compare the curves in figures 6(a) and 6(b). A photograph which would appear either as an identifiable involute (solid curve) or possibly a uniform field of light (dashed curve) in figure 6(a) would appear as a curved arc or a blob of light with the figure 6(b) configuration. With the small gap configuration of figure 6(b), a moving discharge should be detected. This is in accord with the unpublished experimental findings of C. Sorensen, W. Carlson, W. Winovich, and N. Vojvodich of Ames, one photograph of which is reproduced in figure 3. Over a four-order change in pressure and a one-order change in magnetic field and current, a moving, discrete discharge was always detected by the above experimenters.

## The Limiting Case and the Diffuse Discharge

In spite of the fact that the arc of figure 5(a) carried only 12 amperes current, it appears in the photograph to have appreciable width. An increase in current will spread the apparent width of the arc,<sup>1</sup> so that a photograph may show luminosity filling the whole annular region. Increasing the magnetic field will show the same effect by causing the arc to twist more tightly (cf. the solid and dashed curves, fig. 6(a)). As the magnetic field is increased to large values, the parameter  $\alpha$  approaches zero, and the limiting case (eq. (6)) applies. These results predict that with a sufficiently large magnetic field, the discharge should appear relatively uniform and diffuse. The diffuse discharge with large gap and magnetic field has been reported in references 7, 12, 13, and 14. In reference 7 the diffuse discharge is attributed to the use of an incandescent inner electrode operating as a cathode, but the diffuse discharge has been observed when cold copper electrodes were used in references 13 and 14. In reference 12, photographs show an involute at a low magnetic field strength in contrast with a uniform field of light at higher values. In addition to the photographs, Langmuir probes were inserted into the discharge, and their output recorded by oscilloscope and camera. The probes had a substantial direct current component, thereby demonstrating a rather uniform discharge by a means that is completely independent of photography. Reference 12 also contains a theory predicting the diffuse discharge for large gaps and magnetic fields based on considerations completely different from those in the present report.

An interesting limiting case is reported in reference 15, in which a large gap configuration with an extremely large magnetic field (1.8 tesla) produced a discharge in the form of a luminous ring, thereby completely cutting off the electrode current flow.

It is apparent, then, that the diffuse discharge predicted by theory for a large gap with large magnetic fields has been frequently observed.

The theory presented here suggests a gradual transition from a discrete arc to a diffuse one, whereas some experimenters (refs. 12 and 14) have observed an abrupt transition. The theory herein does not take into account the Steenbeck minimum voltage principle (ref. 16) which states that the discharge will always exist in a form which will make its voltage a minimum. Thus since the arc twists more tightly as the magnetic field becomes larger, its length and, consequently, its operating voltage must increase. At some degree of twist, the tightly wound arc may require a higher operating voltage than the diffuse arc; at this point the discharge would change from discrete to diffuse. If the Steenbeck principle is considered, the existence of an arc path described by the dashed curve, figure 6(a), may be questioned, since its long path length may well yield a higher operating voltage than the diffuse discharge.

---

<sup>1</sup>The relationship between arc current, temperature, and diameter is given in reference 11.

## Photography of Electric Arcs

In most cases experimenters have determined the shape of the arc by photography. The experimenter can cope with the usual problems of stopping image movement of high-speed motion with suitable short exposure time, and of preventing overexposure broadening by sufficiently small lens aperture.<sup>2</sup> But more fundamental problems exist. The photograph is sensitive to light; light is not necessarily produced exclusively from the current-carrying region, the arc. Atom recombination, for instance, can produce light in wavelengths to which the camera film responds, and this can be outside of the current-carrying region. Little confusion will exist for low current discharges, such as the 12 ampere discharge of figure 5(a), but those of high current will appear considerably broader in the photograph than the true arc. The time required for atom recombination (and therefore the duration of light) is in the order of 1 millisecond for an arc in ambient environment, so if the arc is driven in a circular pattern at an appreciably greater angular velocity than 1 revolution per millisecond, light may be given off from the whole swept-out region, even though the arc may be discrete. In general, then, photographs of high current, rapidly moving arcs must be examined cautiously.

### CONCLUSIONS

The path of a magnetically rotated electric arc in an annular gap is analyzed and is shown to be the involute of a circle, within the limitations of the chosen simplifying assumptions. The main assumption is that the arc may be thought of as a solid rod conductor, experiencing crossflow aerodynamic drag and being driven by the electromagnetic force. Some published photographs of an arc discharge (with this configuration) appear spiral-like in the annular gap in agreement with the shape predicted by the theory.

Ames Research Center

National Aeronautics and Space Administration

Moffett Field, Calif., July 7, 1964

---

<sup>2</sup>In a private communication, Dr. Erik Soehngen of Wright-Patterson Air Force Base related the following incident to the author. Two independent camera systems, based on short-exposure duration image converter tubes, were set up to photograph an arc discharge of the annular configuration with axial magnetic field. One produced a picture showing a discrete arc, but the other was sufficiently sensitive to respond to the recombination emission in the annular region, and produced a field of uniform light.

## REFERENCES

1. Adams, V. W.: The Influence of Gas Streams and Magnetic Fields on Electric Discharges. Part 1: Arcs at Atmospheric Pressure in Annular Gaps. R.A.E. TN Aero. 2896 (British), June 1963.
2. Angelopoulos, M.: Ueber Magnetisch Schnell fortbewegte Gleichstrombogen. Elektrotech. Z., ETZ-79, 572 (1958).
3. Knabe, W.: Evaluation of Existing Literature on the Interaction of High-Density Plasma with Electric, Magnetic and Fluid-Dynamic Fields. ARL-64-34, Wright-Patterson Air Force Base, Ohio, Feb. 1964.
4. Enkenhus, K.: Results of a Feasibility Study on the Design of a Direct-Current Electric Arc for the NOL Hypervelocity Tunnel No. 9. Naval Ordnance Laboratory, White Oak, Maryland, Nov. 8, 1960.
5. Schuette, H.: Ueber den Einfluss von Stroemungsvorgaengen auf die Lichtbogenwanderung in engen Spalten. Elektrotech. Z., (ETZ) A83, 16 (1962).
6. Burington, R. S.: Handbook of Mathematical Tables and Formulas. Handbook Publishers, Inc., Sandusky, Ohio, 1948.
7. Shepard, C. E., and Winovich, W.: Electric-Arc Jets for Producing Gas Streams with Negligible Contamination. Plasma Jet Symposium, ASME Paper 61-WA-247.
8. Eidinger, A., and Rieder, W.: Das Verhalten d. Lichtbogens in Transversalen Magnetfeld. Arch. El. Tech. 43, 94 (1957).
9. Knabe, W.: A Review of Magnetically Induced Motion. Proc. First Plasma Arc Seminar of the Thermo-Mechanics Res. Lab., ARL 63-151, Wright-Patterson AFB, Ohio, 1963.
10. Walker, R. C., and Early, H. C.: Velocities of Magnetically Driven Arcs in Air and Helium up to 30 Atmospheres. AIEE Winter Meeting, Feb. 1955.
11. Maecker, H.: The Properties of Nitrogen Up to 15,000° K. AGARD Rep. 324, 1959.
12. John, R. R., et al.: Theoretical and Experimental Investigation of Arc Plasma-Generation Technology. Pt. II, Applied Research on Electric Arc Phenomena. Vol. 2, Arc Column Theory, Electrode Materials Behavior and Magnetic Field Arc Discharge Interaction. ASC-TDR-62-729, AVCO Corp., Wilmington, Mass., Jan. 1963.

13. Boldman, D. R.: Arc Jet Chamber Design for a Magnetically Spun D-C Arc. American Rocket Society, Electric Propulsion Conference, March 14-16, 1962, at Berkeley, California, ARS Paper 2349-62.
14. Mayo, R. E., Wells, W. L., and Wallio, M. A.: A Magnetically Rotated Electric Arc Air Heater Employing a Strong Magnetic Field and Copper Electrodes. NASA TN D-2032, 1963.
15. Wilcox, J. M.: Review of High-Temperature Rotating-Plasma Experiments. Reviews of Modern Physics, vol. 31, 1959, pp. 1045-51.
16. Finkelburg, W., and Maecker, H.: Elektrische Bögen und Thermisches Plasma. Handbuch der Physik, vol. XXII, Springer-Verlag, (Berlin) 1956, pp. 254-444.

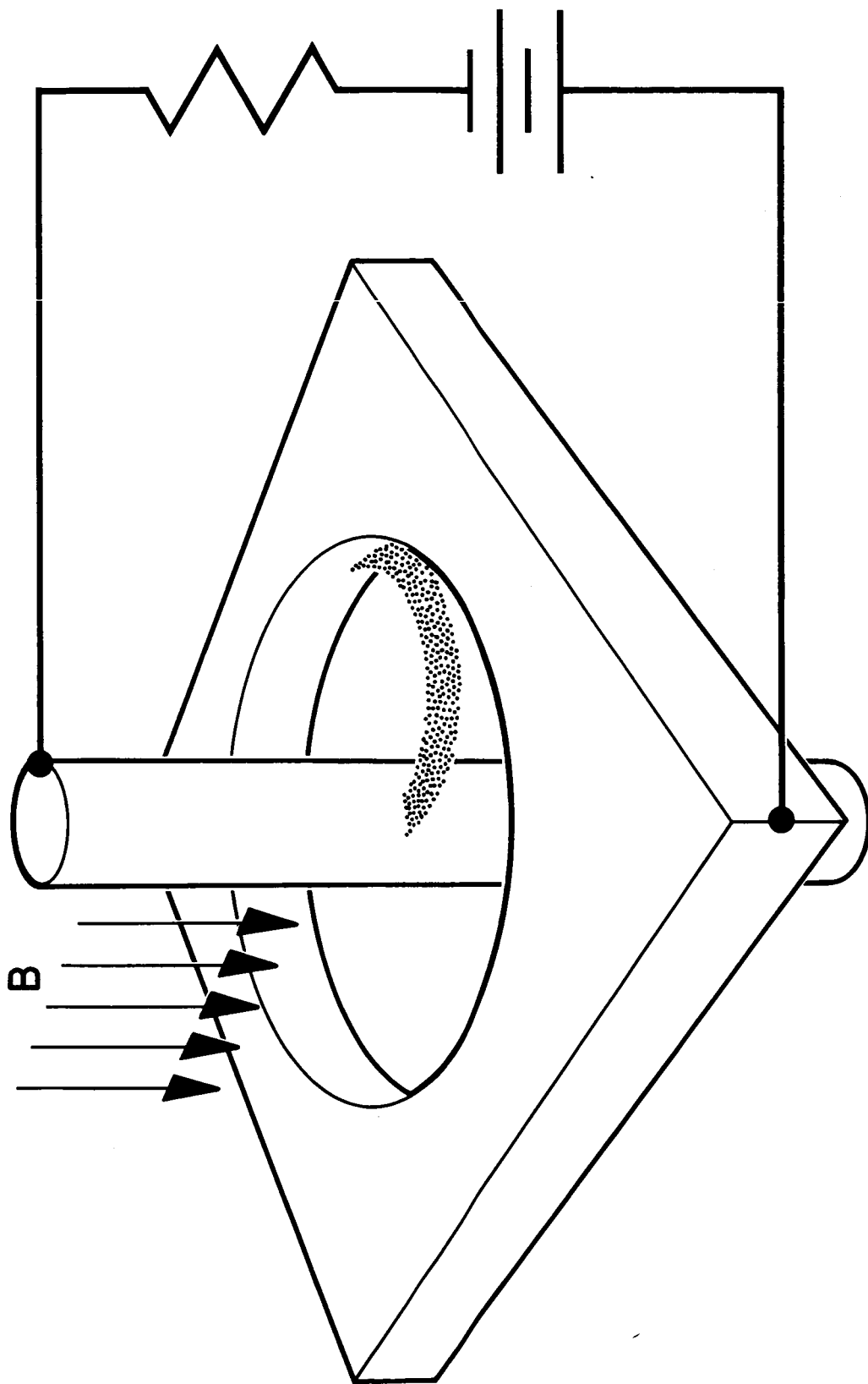


Figure 1.- Annular gap configuration.



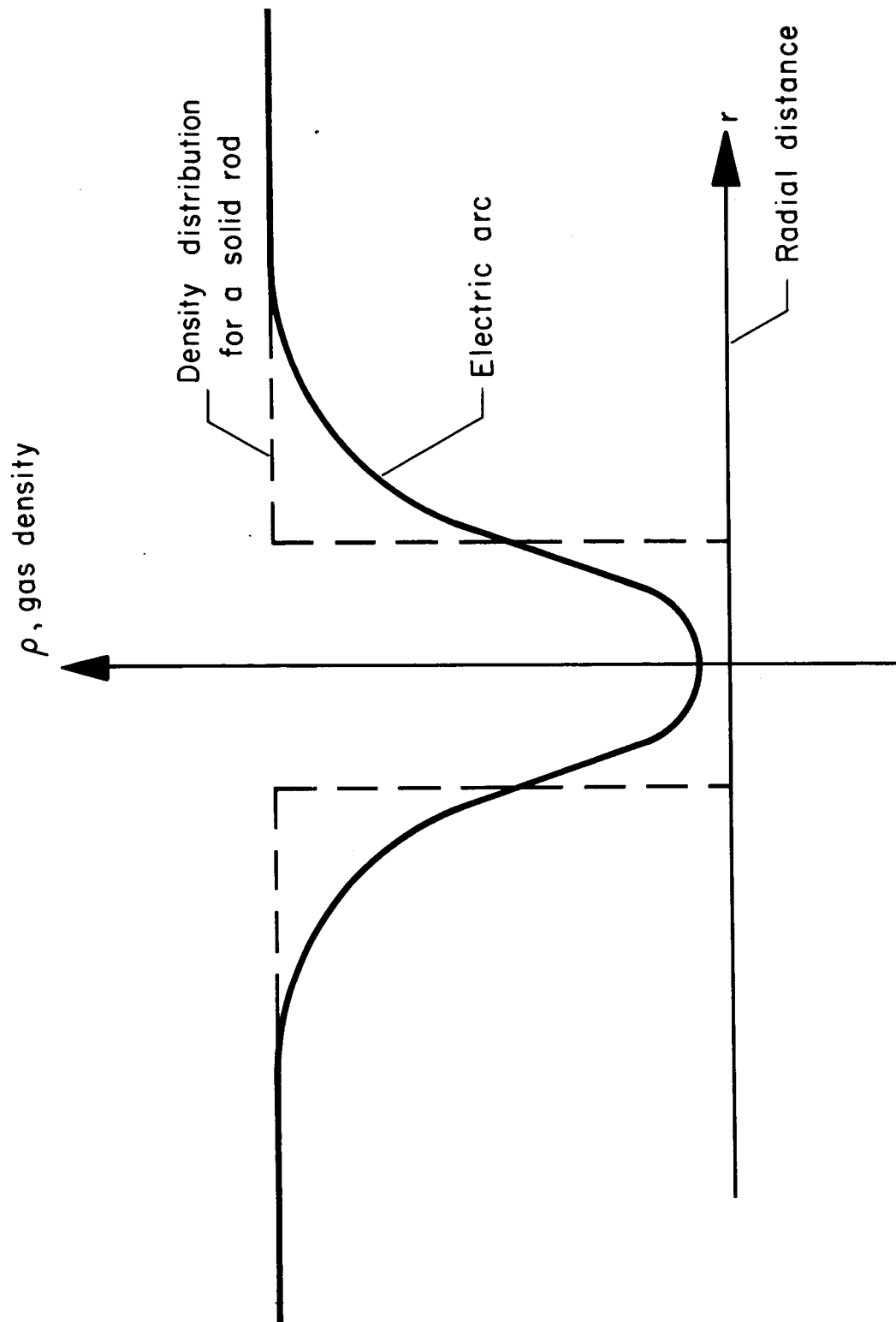
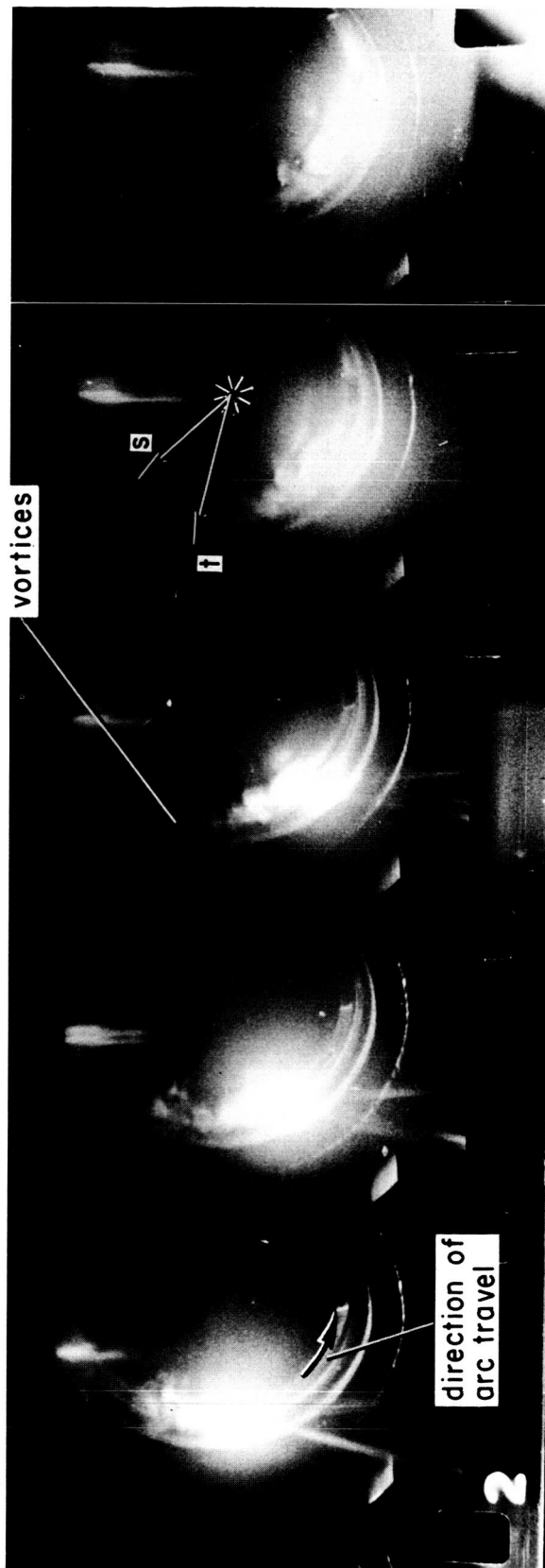


Figure 2.- The impenetrable rod assumption.

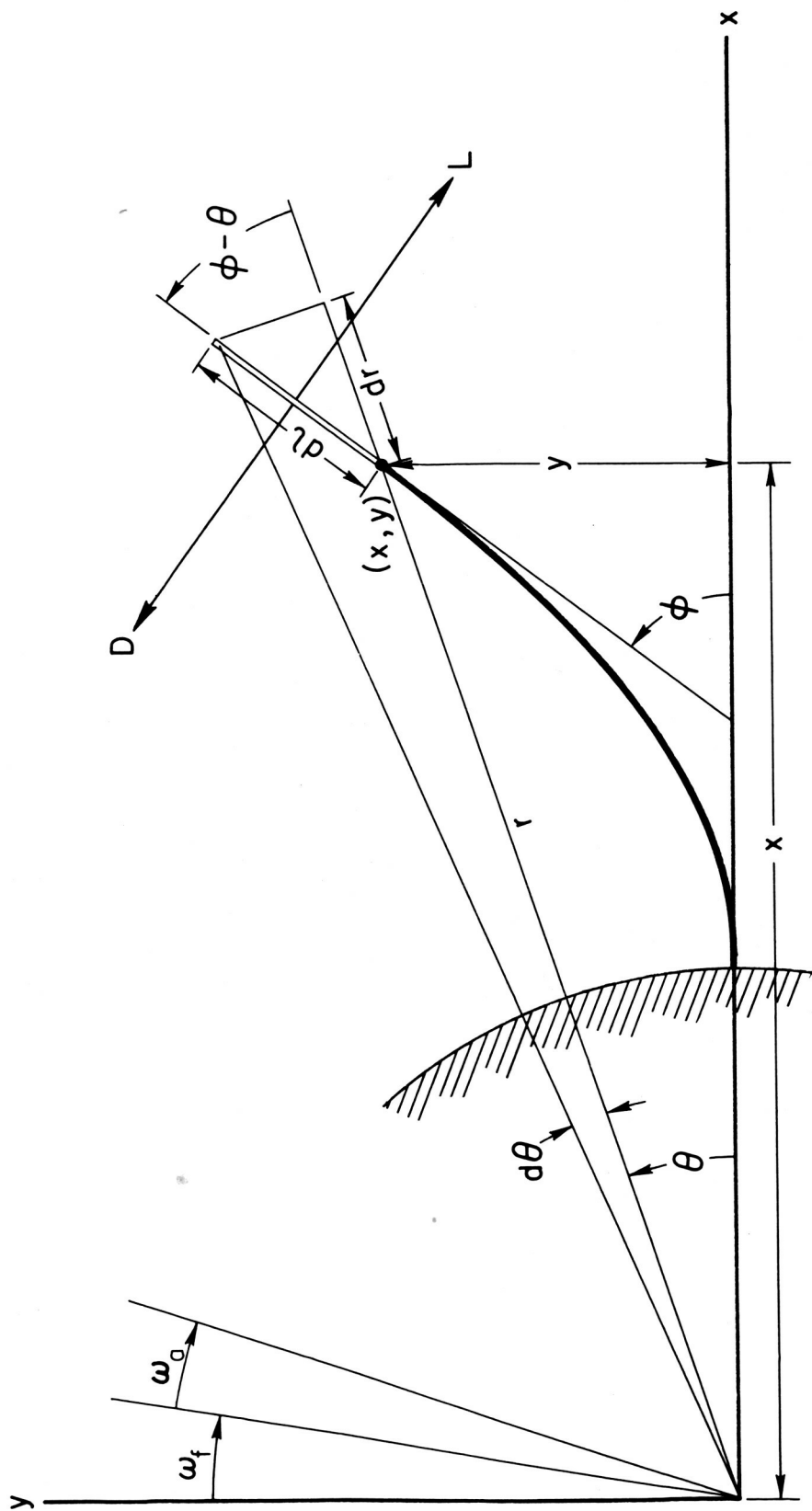


$I = 270$  amperes  
 $B = 0.05$  tesla

$\omega_f + \omega_a = 125$  cycles/second  
 camera speed = 3,000 frames/second  
 $t/s = 1.08$

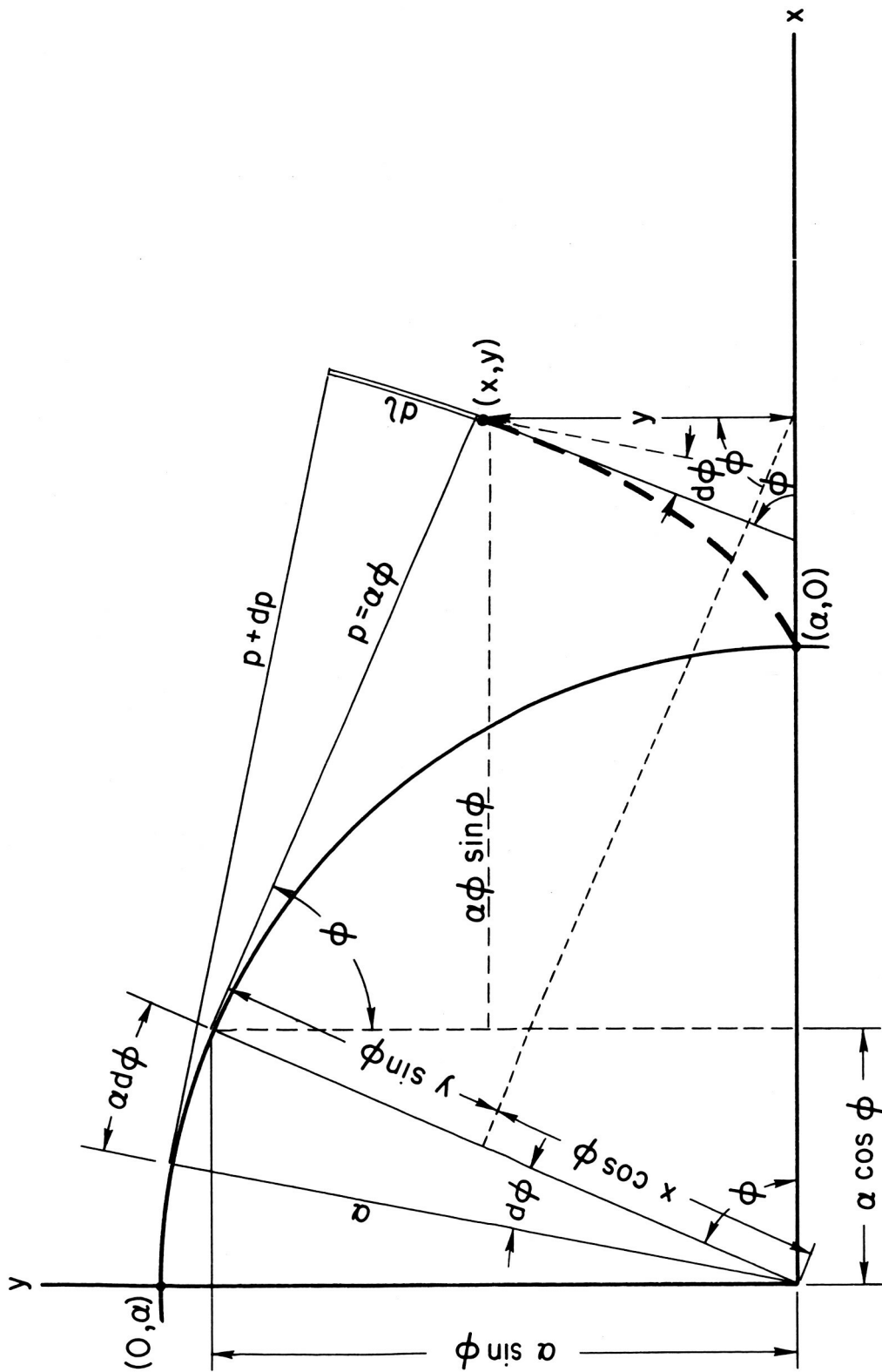
( Unpublished experiment , N.S. Vojvodich )

Figure 3.- Photograph, small gap configuration.



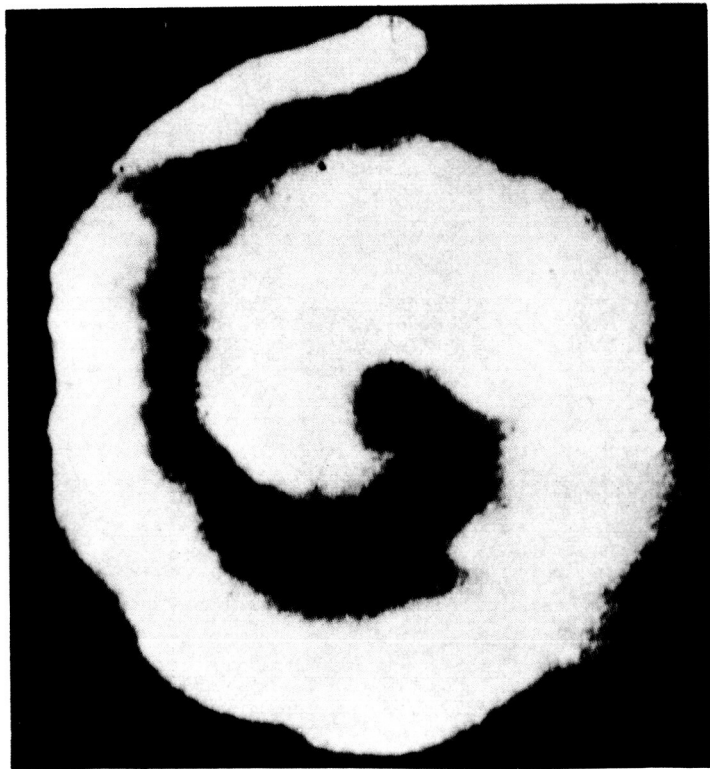
(a) Forces on an arc element.

Figure 4.- Mathematical representation.



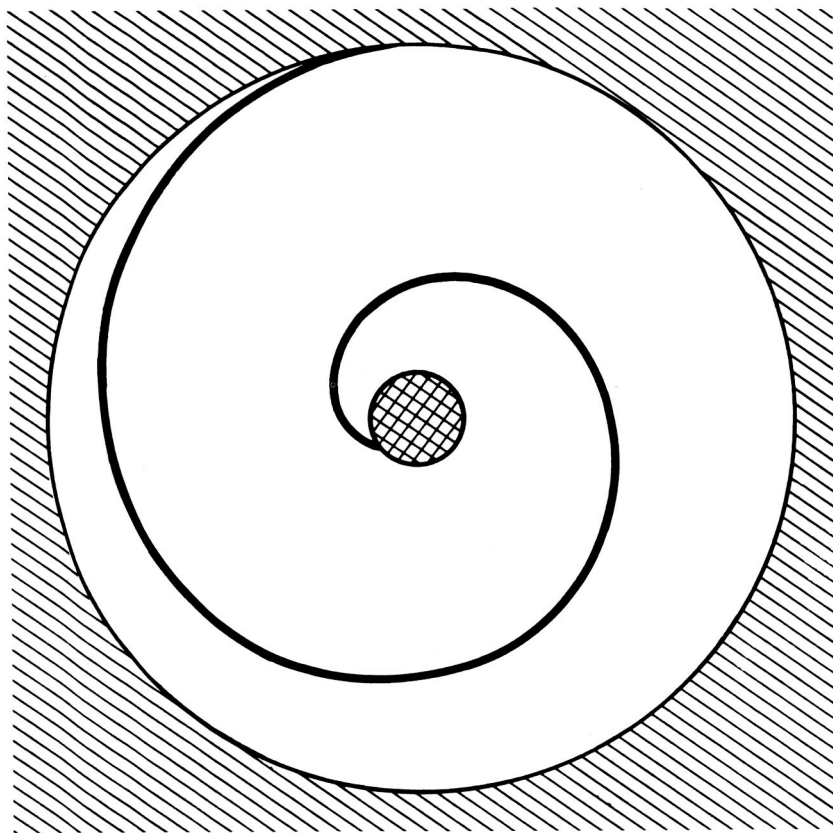
(b) Geometric development.

Figure 4.- Concluded.



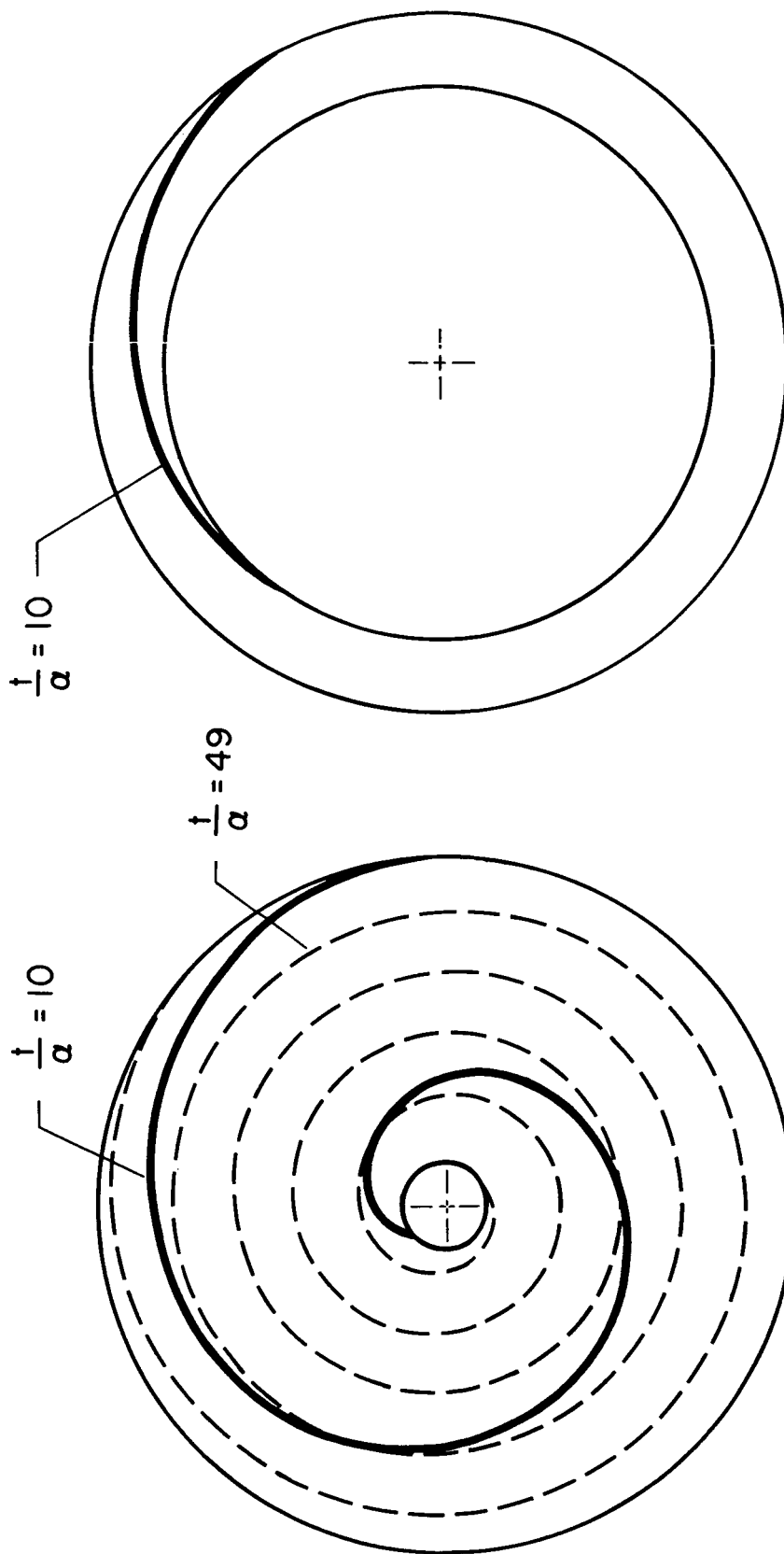
$I = 12$  amperes  
 $B = 0.56$  tesla

(a) Photograph, reference 10.



(b) Calculated curve, with same electrode spacing and number of revolutions as in photograph.

Figure 5.- Comparison of experiment with theory.



(a)  $t/s = 7.75$ .

(b)  $t/s = 1.25$ .

Figure 6.- Effect of gap on appearance of discharge.